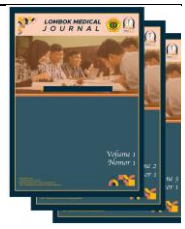
Original article

LMJ 6(1) (2027)

Lombok Medical Journal

http://journal.unram.ac.id/index.php/LMJ



Transcriptomic Analysis of Gallic Acid's Apoptotic Effect on Cervical Cancer Cells

Mochammad Satrio Faiz[1*], Linda Erlina[2], Aryo Tedjo[2]

[1] Master's Programme in Biomedical Sciences, Faculty of Medicine Universitas Indonesia, Jakarta, Indonesia.

[2] Department of Medicinal Chemistry, Faculty of Medicine Universitas Indonesia, Jakarta, Indonesia

DOI: https://doi.org/10.29303/8s1sqc52

Article Info

Received : **30 June 2026**

Revised : **12 August 2026**

Accepted : **28 October 2026**

Abstract: This study investigates gallic acid's (GA) anticancer effects on HeLa cells by analyzing gene expression changes over time. An analysis was performed using transcriptomic data from HeLa cells treated with 50 µg/mL of GA at four different time points (2, 4, 6, and 9 hours) sourced from the GEO database. Predictive machine learning model for GA's IC_{50} value was developed, and molecular docking with catalase was performed. Analysis revealed 4013 differentially expressed genes, narrowed down to 288 genes that were consistently regulated across time points, with TNF identified as the key hub gene, showing significant fold increases. The predictive model estimated an IC_{50} value of 46.376,71 nM for GA, and the following docking indicated favorable binding interactions with catalase. These in-silico findings suggest GA's potential as an anticancer agent by promoting TNF-mediated apoptosis in HeLa cells, warranting further in-vitro validation and exploration of its therapeutic potential. Translational potential of GA in cervical cancer remains speculative as there are absence of robust human pharmacokinetic data for GA.

Keywords: Gallic Acid, Apoptosis, Transcriptomics, HeLa Cells, Cervical Cancer

Citation: Faiz, M. S., Erlina, L., & Tedjo, A. (2027). Transcriptomic analysis of gallic acid's apoptotic effect on cervical cancer cells. *Lombok Medical Journal*, 6(1), 23-33. https://doi.org/10.29303/8s1sqc52

Introduction

Cervical cancer remains a leading cause of cancer-related mortality among women globally, with GLOBOCAN 2022 estimating 662,301 new cases and 348,874 deaths worldwide in 2022, nearly all of which are attributable to persistent infection with high-risk human papillomavirus (HPV) (Z. Li et al., 2025). This burden is particularly skewed toward low- and middle-income countries, which account for most of cervical cancer deaths. Southeast Asia has been identified as one of the regions bearing a disproportionately high share of this burden (Setiawati et al., 2026). Cervical cancer remains a major global health challenge, with standard treatments such as surgery, radiotherapy, and platinum-based chemotherapy providing disease control in many cases but often at the cost of substantial toxicity, treatment resistance, and recurrence that impair quality of life for survivors (Chimento et al., 2023; Pescinelli et al., 2025).

Plant-derived compounds, particularly polyphenols, have emerged as promising adjuncts because they act on multiple cancer-relevant pathways, can sensitize tumor cells to conventional therapies, and frequently exhibit selective cytotoxicity toward cancer cells with potentially lower normal tissue toxicity and has thus experienced a surge in usage trend (Chimento et al., 2023; Seca & Pinto, 2018). The use of these plant-based compounds deemed 'phytotherapy' has been widely recognized as an alternative method in cancer treatment in various countries. Studies showed that there are more than 3,000 plant species that elicit potential anti-cancer activities. Data from the Food and Drug Administration (FDA) supports this trend, showing as many as 40% of drugs in the US market are

Email: satrio.faiz.g@gmail.com

Copyright © 2027, The Author(s).
This article is distributed under a Lisensi Creative Commons Atribusi 4.0 Internasional.

products of either natural compounds or synthetic compounds inspired by natural ingredients, and 74% of them has had been applied in standard anti-cancer therapy. Some compounds that are widely used currently include vincristine which is an alkaloid compound extracted from the leaves of *Catharantus roseus*, paclitaxel a terpenoid from the bark of the Pacific Yew tree (*Taxus brevifolia*), and homoharringtonine another alkaloid from the Japanese Plum Yew. Other potential compounds currently undergoing clinical trials include ingenol mebutate, a terpenoid from *Euphorbia peplus*; curcumin, a phenolic sourced from turmeric (*Curcuma longa*); and betulinic acid from *Gratiola officinalis* (Seca & Pinto, 2018).

Plants allow the efficient and economical acquisition of natural compounds, as the synthesis of secondary metabolic compounds in the laboratory setting is not always feasible. These metabolites are small organic compounds produced by an organism that are not essential for the growth, development, or reproduction of the said organism. The diversity of secondary metabolites can be classified generally into three main categories: terpenoids, phenolics, and alkaloids. Plant-derived secondary metabolite compounds can often be used as lead compounds in the development of new drugs. Many secondary metabolite compounds have been used as active ingredients for drugs and many other new compounds are consistently discovered, which undoubtedly can expand the scope, and familiarize the masses to the potential of plant derived compounds as pharmaceuticals (Seca & Pinto, 2018).

One of the most promising secondary metabolic compound is gallic acid (GA), a phenolic compound that exhibit anti-oxidant, anti-inflammatory, anti-viral, anti-bacterial and have also been confirmed to also elicit anti-cancer properties (Indrayanto et al., 2021; Khorsandi et al., 2020; Lee et al., 2017; Moghtaderi et al., 2018). This potential is demonstrated by its ability to induce apoptosis and inhibit the proliferation of cancer cells, which are one of the key characteristics of anti-cancer drugs (Seca & Pinto, 2018), against various types of cancer, such as breast, cervical, colorectal, liver, lung, skin, leukemia and lymphoma. Research showed that GA's anti-cancer activity is not accompanied by detrimental effects that usually exist as a side effect with the use of standard chemotherapeutics such as anthracycline, platinum-based agents, or taxanes. The anti-cancer activity of GA has especially been studied in MDA-MB-231 breast cancer cell line where apoptosis was induced through the P38MAPK/P27/P21 signaling pathway (Lee et al., 2017), ferroptosis through the production of reactive oxygen species (ROS) (Khorsandi et al., 2020), and also along with the administration of curcumin, another phenolic compound, seems capable to induce apoptosis by reducing Bcl-2 expression and increasing Bax, cleaved-caspase3, and PARP, which are intrinsic apoptotic pathway proteins (Moghtaderi et al., 2018). Additionally, GA also shows some protective activity against lymphocytes and also antioxidant effect on normal cells (Lee et al., 2017), both of which indicate selective toxicity against cancer cells. This selectivity is also reinforced by the fact that there was no evidence of significant changes in fibroblast viability (Moghtaderi et al., 2018).

GA is a compound that can be found in many fruits, green tea (*Camellia sinensis*), red wine, and especially in gallnut seeds (*Terminalia chebula*). This ease of acquisition supports GA's validity as a potential anti-cancer as it will simplify and speed up the isolation and extraction process, enabling cheaper and faster drug design and manufacturing processes.

In cervical cancer in-vitro models, GA and GA-rich plant extracts have shown activity against HeLa cells and can enhance the efficacy of standard regimens (e.g., cisplatin), supporting the rationale for integrating plant-based adjuvants into cervical cancer therapy (Hasmah Abdullah et al., 2026). This evidence justifies investigating GA in HeLa cells not only as a direct anticancer agent but also as a potential chemo-sensitizer or tolerability enhancer when used alongside conventional cervical cancer therapies, though most of these are limited to preclinical evidence.

GA exerts well-documented antitumor activity in HeLa cervical cancer cells through p53/Bax/caspase-dependent apoptosis, ROS-mediated oxidative stress, and ferroptosis characterized by lipid peroxidation (Hasmah Abdullah et al., 2026; Wu et al., 2022). Despite this, bioinformatics analysis of GA's targets has only been confined to colorectal cancer and glioma and has not yet been applied particularly to cervical cancer.

In this study, an in-silico analysis was done to assess changes in cancer cell gene expression due to the administration of GA. The analysis was based on data from a transcriptomic study of HeLa cells by Tang *et al* (2021) obtained from the Gene Expression Omnibus (GEO) database. Data analysis was carried out bioinformatically via gene profiling, pathway enrichment analysis, and determination of hub genes, then continued with the creation of activity prediction model of GA using chemoinformatic methods and ended up with the validation of the compound activity through molecular docking.

Materials and Methods

Data acquisition, cleaning, and annotation

This analysis was based on the dataset by Tang et al. (2021) with accession number GSE158788. The study carried out gene expression profiling of 15 samples that

are treated by GA at a dose of 50 µg/mL which was then observed at 4 different observation time points, GA_2, GA_4, GA_6, GA_9 which corresponds to the 2nd, 4th, 6th, and 9th hour, with GA_0 as the control. The RNA-seq process was carried out using the Illumina HiSeq 4000 platform. Data processing for this analysis was initially carried out using the GEO2R statistical package, by comparing the expression levels between each observation time point and control. The significance level was set at p-value=0.05 with false discovery rate adjustment (Benjamini-Hochberg method). The output in the form of tabular data of the gene fold changes, volcano plot, uniform manifold approximation and projection (UMAP) plot, and Venn diagram of DEG at each time point, were downloaded so that data cleaning can proceed. Data cleaning was then carried out by excluding genes that had inconsistent increased/decreased values between those observation time points using the Python Data Analysis Library (pandas). The selected genes were annotated using Enrichr with the KEGG 2021 Human reference database. Several metabolic pathways from KEGG terms were selected according to relevance and then annotated to STRING to view the protein-protein interaction (PPI) network. The output data from STRING in. tsv format was then used to build a metabolic pathway network to determine the hub genes.

Gallic acid in-vivo activity prediction modelling

The activity prediction model for one of the selected hub genes (i.e. TNF) was then built using Osiris DataWarrior software. It was done by selecting the upstream signaling pathway enzymes that possibly contribute to the expression of TNF from the ChEMBL database. Then, data curation was carried out by excluding measurement types other than the IC50. Descriptors were then calculated using SkelSpheres and clustering was carried out with a similarity threshold of 80% based on these descriptors. Representative molecules will be classified as the training set for model training, while non-representative molecules will be used as the validation set. The model was trained with the Support Vector Machine (SVM) regression algorithm based on $\log IC_{50}$ data, with default parameters (gamma=0, epsilon=5, kernel=2, c=130.0). Model evaluation was carried out by previously calculating Ligand Efficiency Dependent Lipophilicity (LELP), the value of which was obtained from counting atoms from the structure of each molecule along with the IC_{50} value from the $\log IC_{50}$ prediction results. Model selection was based on the best R2 value.

Validation of the prediction through molecular docking

The 3D structure of the target protein, catalase, was downloaded from Protein Data Bank (PDB) while the 3D structure of GA was downloaded from PubChem. Protein and ligand preparation, and docking were done with Molegro Virtual Docker (MVD) software. First, redocking was carried out on the protein and its native ligand to determine the optimal grid coordinates for the actual docking. The default scoring function (i.e. MolDock Score (GRID)) of the docking process was selected. 2x20 docking runs were carried out with the first 20 runs based on the cavity coordinates and the second 20 runs based on the reference ligand coordinates. Results showed cavity-based redocking yield poses with lower binding energy, and thus better. Docking of GA to the target protein was then carried out using the grid coordinates that yields the lowest Root Mean Square Deviation (RMSD) value.

Results

Through data exploration using the R statistical package, 4013 DEGs were detected. Filtering was carried out on these DEGs resulting in 288 genes that experienced constant regulation over time (either increased or decreased). The filtered genes were then annotated to KEGG database which yields 211 KEGG terms which were then selected into 20 high relevance terms related to cancer signaling pathway. Protein interaction mapping for each term was carried out with STRING and comprehensively combined in the pathway interaction network as shown in supplementary figure 1. The resulting interaction network shows 10 genes that are central to 20 previously selected cancer-related signaling pathways, with six of them showing decreased expression while the other four showing increased expression. TNF was shown as the most significant of these genes, where it acts as a hub gene that connects 6 different signaling pathways related to cell death, making it one of the most prominent genes in this analysis. The fold change (FC) of TNF and other less prominent hub genes can be seen in table 1.

The creation of an SVM-based machine learning model to predict GA activity was achieved through data wrangling from IC50 values dataset for TNF from CheMBL database. The evaluation metric of the model is based on LELP value which is a concept that combines ligand efficiency (LE) and lipophilicity (LogP) into a singular unitless value, and can be used as a strong predictor for drug-likeness in-vivo from an in-vitro data (Rackham et al., 2014). LELP can be calculated using the formula LELP = $LogP - \frac{\Delta G}{N}$ where the value of N was automatically obtained from the software's descriptor calculation and ΔG obtained from the formula ΔG =

$RTln(K_i)$ where $K_i \approx IC_{50}$ is assumed. The validated model was then used to predict the $logIC_{50}$ value of GA which yielded the result of 4,6663, equivalent to the IC50 value of 46.376,71 nM. LELP value of GA can then be subsequently calculated to be 0,21718.

Molecular docking was then carried out using the crystal structure model of catalase with its native ligand (PDB ID: 1DGF). Catalase was selected as the target protein because it plays a key role in oxidative stress, a condition intensified by its inhibition via GA (Chang et al., 2015). Determining the optimal binding site grid was conducted by first redocking the native ligand, NADPH, to catalase. The optimal grid was determined to be the cavity coordinates X: 27.86; Y: 73.58; Z: 70.40 with the best pose resulting in RMSD value of 1.76. Rerank score was used as the main evaluation parameter, which is a modification of the MolDock score with the addition of some additional energy terms. Docking results can be seen in table 2.

Table 1. Identified Hub Genes and Their Fold Change in Each Time Point of Observation

Hub genes	Log_2FC				Regulation
	GA_2 vs GA_0	GA_4 vs GA_0	GA_6 vs GA_0	GA_9 vs GA_0	
TNF	1.546	2.275	2.535	3.022	UP
EDN1	1.681	1.607	0.977	0.658	DOWN
SOCS3	1.689	1.672	1.321	1.277	DOWN
PTEN	-0.267	-0.316	-0.34	-0.825	DOWN
FGFR1	0.469	0.629	0.68	0.819	UP
WNT5A	-0.227	-0.289	-0.366	-0.658	DOWN
WNT7B	0.408	0.319	0.316	0.279	DOWN
FZD1	0.518	0.485	0.419	0.184	DOWN
FZD7	2.152	1.733	1.696	1.695	DOWN
CSNK1E	0.271	0.377	0.399	0.57	UP
TPTEP2-CSNK1E	0.269	0.375	0.399	0.578	UP

Table 2. Molecular Docking Result of Catalase with its Native Ligand and Gallic Acid Sorted by Rerank Score

Run Identifier	Ligand	MolDock Score	Rerank Score	HBond
[00]NDP_4000 [A]	NDP_4000 [A]	-244.877	-154.304	-14.1163
[02]NDP_4000 [A]	NDP_4000 [A]	-231.872	-140.955	-10.4546
[01]NDP_4000 [A]	NDP_4000 [A]	-237.724	-135.069	-13.827
[03]NDP_4000 [A]	NDP_4000 [A]	-231.702	-108.62	-7.84544
[00]GALLIC_ACID	GALLIC_ACID	-93.3889	-79.7025	-12.7568
[01]GALLIC_ACID	GALLIC_ACID	-90.2808	-77.5606	-9.80687
[04]GALLIC_ACID	GALLIC_ACID	-80.1863	-70.7503	-9.94426
[02]GALLIC_ACID	GALLIC_ACID	-79.0798	-69.9956	-7.7373
[03]GALLIC_ACID	GALLIC_ACID	-78.8436	-69.6166	-11.6746
[04]NDP_4000 [A]	NDP_4000 [A]	-229.641	-49.0911	-18.1489

Venn diagram depicting the DEG between different time points of observation and its intersections can be seen in figure 1. The existence of 4013 DEG genes indicates that there are core genes that are consistently affected by GA which are important for analysis at the next stage. In addition, each time point has a unique number of DEGs that can indicate the presence of time-related dynamics of gene expression responses. DEG with the highest number is at the intersection of GA_4 and GA_9, with 1857 genes, indicating that the response that occurred at GA_4 was also important at GA_9 which could also indicate the presence of a secondary response. Meanwhile, observations of DEGs obtained in GA_6 where there are only 294 genes, may indicate a transition phase in cellular response. Intersections that occur at other observation times may provide additional insights into time-related progression of DEGs, where a series of genes are sequentially activated or repressed. The clustering seen in the UMAP plot (figure 2), shows a progressive divergence of gene expression as treatment time increases. Visualization of the progression can also be seen relatively easily where the

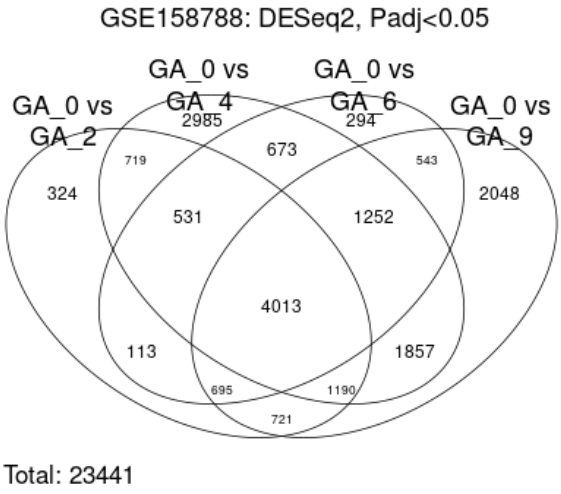


Figure 1. Venn Diagram of The Intersection of DEG Between Observation Time Points

GA_9 cluster points are seen much further from other observation time clusters, which indicate significant changes in gene expression at that observation time point. Meanwhile GA_2, GA_4, and GA_6 cluster are relatively closer to the GA_0 cluster. These results indicate the possibility of a gradual transition of cellular responses as treatment time increases.

Discussion

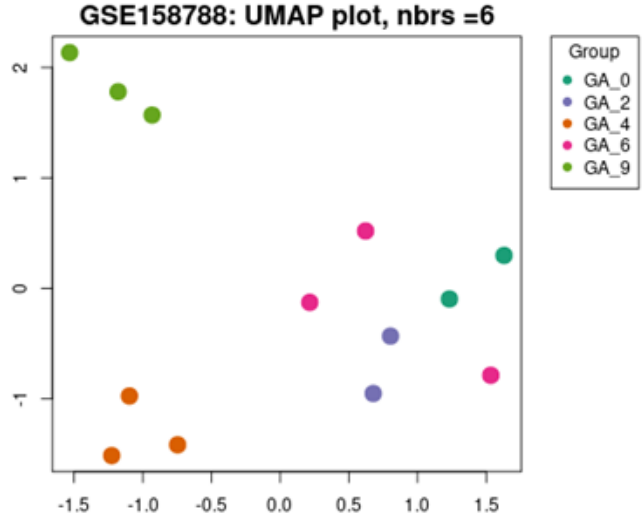


Figure 2. UMAP visualization of PCA-reduced DEGs

The SVM-predicted IC_{50} of approximately 46.4 µM for GA's TNF-related activity appears to fall within a plausible range when compared with experimental data, though considerable variability exists across studies depending on assay conditions and exposure duration. Ozan et al. reported IC_{50} values for GA alone in HeLa cells of 289.4 µM at 24 h and 174.7 µM at 48 h using the MTT assay. These values are substantially higher than the 46.4 µM prediction; however, the selectivity index at 48 h was 2.55, indicating preferential toxicity toward cancer cells (Ozan et al., 2026). Sarı et al. similarly evaluated GA in HeLa cells and reported a 48-h IC_{50} of 239.2 µM, noting that the IC50 value in GA acid-treated HeLa cells exhibited a decrease with increasing exposure time (Sarı et al., 2024). These two studies consistently place the pure GA IC_{50} in HeLa cells in the range of approximately 170–290 µM depending on incubation time, which is notably higher than the 46.4 µM prediction. However, an earlier study by Ismail et al. reported that GA possessed "inhibitory activity against the tested cell in a dose-dependent manner, with an IC50 of 80 µM using MTT assay" in HeLa cells. This value is closer to the predicted 46.4 µM. Additionally, the same review noted that GA at doses of 10, 15, and 20 µg/mL (approximately 59–118 µM) "remarkably inhibit cell migration" in HeLa cells. also confirmed that "gallic acid has been shown to significantly decrease HeLa cell viability in a dose-dependent manner" (Ismail et al., 2021). The discrepancy between the predicted 46.4 µM and the experimentally observed values (80–290 µM) may be explained by the fact that the SVM model was trained on ChEMBL IC_{50} data for TNF-related activity specifically, rather than general cytotoxicity. Notably, Ozan et al. demonstrated that GA combined with cisplatin achieved combination index values of 0.61 to 0.92, indicating synergistic interactions, and that cytokine profiling showed modulation of pro-inflammatory cytokines including increased IL-10 levels. This suggests that GA's effects on TNF-related pathways may occur at concentrations lower than those required for outright cytotoxicity.

Several studies have employed molecular docking to investigate GA's interactions with cancer-related proteins. Tedasen et al. performed network pharmacology and molecular docking analyses of Triphala extract, in which GA was identified as the predominant phenolic compound by LC-MS. Their network pharmacology analysis ranked PPARG, PTGS2 (COX-2), EGFR, MMP9, TLR4, ACE, REN, PPARA, SERPINE1, and MMP2 as top hub proteins involved in oxidative stress, inflammation, and metabolic signaling pathways. While their docking focused on kynurenic acid rather than GA specifically, the study established that Triphala-derived compounds (including GA) target oxidative stress response and inflammatory signaling pathways, with binding affinities below −7.0 kcal/mol reported for key interactions. This supports the biological plausibility of GA binding to oxidative stress-related targets such as catalase (Tedasen et al., 2026). Another molecular docking study conducted by Meem et al. targeting caspase-3, COX-2, and other cancer-related proteins, reporting strong ligand-target interactions for compounds from an extract containing phenolic derivatives. Their study evaluated cytotoxicity on HeLa cells and demonstrated strong antioxidant activity (IC_{50}: 31.49 and 48.94 µg/mL for DPPH and ABTS assays) (Meem et al., 2026). The docking results in the present study showing GA binding to catalase at the NADPH site with engagement of residues Arg 203, Asn 149, Gln 195, Phe 198, and Ser 201 represent a possible novel finding. The NADPH binding site of catalase is a well-characterized regulatory region, and binding at this site could plausibly inhibit catalase's antioxidant function. The negative rerank score obtained is consistent with favorable binding, comparable to the negative binding energies reported in other docking studies of phenolic compounds against oxidative stress targets.

TNF as a hub gene with roles in 6 different pathways related to cancer cell apoptotic signaling, exhibits an increase in expression at each observation time after GA administration. This may indicate a

central importance of the gene in inhibiting cancer cell progression. TNF has been shown to trigger apoptosis associated with NF-κB inhibition. TNF that is bound to TNFR1 can trigger the recruitment of the adapter protein TNF-associated receptor death domain (TRADD) which will bind to TNF receptor-associated factor 2 (TRAF2) and kinase receptor-interacting protein 1 (RIP1), which in turn will then recruit IκB kinase (IKK). IKK in turn will phosphorylate and trigger IκBα degradation. This makes it possible for NF-κB to translocate to the nucleus which is normally inhibited by IκBα (Yuan et al., 2022). The NF-κB signaling pathway generally promotes survival and cellular inflammatory response, but TNF is a known pleiotropic cytokine that can also initiate signaling pathways associated with increased apoptosis. RIP1 which binds to the TNF-TNFR1 complex can dissociate caused by the activity of the de-ubiquitination enzyme CYLD. This dissociation allows the formation of a RIP1 complex with Fas-associated death domain (FADD) and caspase-8 as an apoptotic effector. Another important fact is that TNF also plays a role in the necroptosis signaling pathway in conditions where the aforementioned apoptosis pathway is someway inhibited. In this condition, RIP1 will form necrosomes as a cell death effector together with RIP3, facilitated by the RIP homotypic interaction motif (RHIM) domain (Chang et al., 2015).

Several reviews synthesizing pathway-level mechanisms across multiple phenolic compounds corroborate that TNF/NF-κB and death-receptor signaling consistently emerge among the top-affected pathways in polyphenol-treated cancer cells, lending support to the plausibility of TNF serving as a hub gene in the present dataset. Fakhri et al.'s systematic review of TLR/NF-κB/NLRP signaling modulation by bioactive phytocompounds explicitly frames TNF-receptor superfamily members CD95(Fas)/APO-1 and TRAIL as initiators of death-inducing signaling complexes that recruit caspase-8, and documents that EGCG inhibits TNF-α expression while other polyphenols (gallotannin, ellagic acid, fisetin, astragalin) inhibit proliferation and invasion of several cancer types via modulation of TNF-α, iNOS, and NF-κB signaling (Fakhri et al., 2022), which underscores this pathway as a recurrently targeted convergence point for phenolic compounds across cancer types. Bakrim et al.'s review of dietary phenolic anticancer mechanisms similarly emphasizes that polyphenols broadly activate NF-κB, AP-1, PI3K/Akt, and MAPK signaling cascades, while documenting the specific case in which caffeic acid phenethyl ester blocks NF-κB activation by inhibiting both TNF-α- and paclitaxel-induced NF-κB signaling in prostate cancer cells, alongside downregulation of apoptosis-inhibiting proteins cIAP-1, cIAP-2, and XIAP (Bakrim et al., 2022). The same research from Bakrim et al. also note that curcumin represses TNF-α-induced NF-κB nuclear translocation by suppressing IκBα phosphorylation, an opposite effect to the apoptosis-promoting TNF upregulation reported for GA and quercetin in HeLa cells (Bakrim et al., 2022). This dual capacity of phenolic compounds to either activate or suppress NF-κB/TNF signaling depending on cellular context and compound structure is an important nuance, and the progressive TNF fold-change increase observed in the present study (1.55→3.02) should be interpreted as consistent with the pro-apoptotic, rather than the anti-inflammatory/NF-κB-suppressive, branch of polyphenol action documented in cancer cells.

The relationship between TNF and TGF-β has been discussed extensively by (Liu et al., 2021). In general, TNF and TGF-β act as counterbalance, that is, both can increase each other's expression or inhibit each other instead. However, the function and action of TNF and TGF-β are strongly influenced by the cellular context in which these two cytokines are located. For example, in the context of apoptosis, the two synergistically induce apoptosis in Schwann cells, SNU620 gastric cancer cells, oligodendrocytes, and human umbilical endothelial cells by inducing the expression of apoptotic proteins. However, both can also provide synergistic inhibition of apoptosis, for example in hepatic stellate cells by reducing the apoptotic gene CD95L expression and inducing NF-κB activation. This fact is complicated by the mutually antagonistic nature of these two cytokines. For example, in epithelial cells, TGF-β induces cell apoptosis, while TNF can induce the anti-apoptotic protein P21 to regulate apoptosis, as well as antagonism found in melanocytes, splenocytes, osteoblasts (Liu et al., 2021). It can be concluded that these two cytokines have multiple roles in the regulation of cell proliferation, so extrapolating these facts into the context of this research is difficult, as in this study, there was an increase in TNF expression in HeLa cells.

Research from (Sivaprasad & Basu, 2008), revealed the involvement of the autophagy process which increases cell death mediated by ERK1/2 (MAPK) which can be induced by TNF. The autophagy process itself has a dual role in cellular processes, that it can act as an inhibitor or potentiator of cell death. In the HeLa cervical cancer cell line, autophagy was demonstrated to be a process that precedes apoptosis through multiple mechanisms (Dasari et al., 2020; Gámez-García et al., 2021; L. Li et al., 2021; Xu et al., 2021). TNF is known to activate ERK1/2 directly through its cascade of downstream signaling pathways. Sivaprasad et. al. stated that pharmacological inhibition of ERK1/2 actually reduces autophagy ability and increases TNF-induced apoptosis. In other words, autophagy is actually a protective mechanism against TNF-induced apoptosis. This observation was demonstrated in several

cancer cell lines such as MCF-7 breast cancer and H29 colorectal cancer cells. (Sivaprasad & Basu, 2008). At first glance, these two facts are contradictory, this is because the autophagy process acts as an intermediary process before apoptosis occurs. In conditions of increased TNF expression as in this study, the autophagy mechanism which is also increased due to ERK1/2 activation may not be sufficient to counteract apoptotic signals from TNF, so that the relationship between TNF and ERK1/2 on apoptosis becomes linear.

The interaction of TNF and the sphingolipid signaling pathway is complex with dual effects, where TNF can trigger an increase in pro-apoptotic molecules from this pathway, namely ceramide and sphingosine, through activation of death receptors such as TNFR1, Fas, and TRAIL; and can also trigger the synthesis of anti-apoptotic molecules such as SphK1/2 and S1P (Sukocheva et al., 2024). The existence of this dual effect suggests the complexity that occurs in conditions of TNF overexpression. The implications of this event will probably depend on several factors, namely the level of expression of TNFR 1/2 and the ability of each cell to respond to signals produced by this receptor, the condition where cells are damaged or under physiological stress will be more likely to respond to the direction of the apoptotic pathway, the presence of other cytokines that can increase or reduce the function of TNF, as well as the expression level and activity of enzymes in the sphingomyelin pathway such as sphingomyelinase and SphK1. Food-derived polyphenols have been shown to be able to regulate TNF-α/NF-κB signaling axis, suppressing NF-κB nuclear translocation while concurrently upregulating death receptors such as DR5 to sensitize cancer cells to apoptosis (Dinislam et al., 2026; Pandey et al., 2025; Sharif et al., 2026). Despite these facts, it turns out that the effects of these food-derived compounds on the sphingolipid signaling pathway and their interactions with the TNF signaling network are still not well known and only a few of these natural ingredients are known to influence these two signaling pathways. Sukocheva et. al. (2024) gave an example of a compound that has been widely studied, apigenin, which together with TNF can stimulate apoptosis in colorectal cancer cells, HepG2 and Huh-7 cells (hepatocellular carcinoma), prostate cancer cells and also lung cancer cells. In breast cancer, this compound has dual effects, where at low doses apigenin actually stimulates the development of cancer cells. Other secondary metabolite compounds that yield an inhibitory effect on SphK1 and sensitize cancer cells to the pro-apoptotic effects of TNF are epigallocatechin gallate (EGCG), resveratrol, and quercetin (Sukocheva et al., 2024). In other words, it does not rule out the possibility that GA, which is also part of the phenolic group of secondary metabolite compounds, shows the same activity, especially since in this analysis GA was proven to increase TNF expression.

Regulation of TNF expression is complex, stimulus dependent, and occurs at the transcriptional, post-transcriptional, translational, and post-translational levels, involving multiple enzymes, molecules, from multiple signaling pathways. One of the mechanisms for increasing TNF expression is through the induction of oxidative stress by inhibition of catalase activation and depletion of glutathione (GSH) which ultimately causes necroptosis (Chang et al., 2015). Based on this information, molecular docking of GA was performed on catalase as one potential mechanism that could explain the increase in TNF expression in the context of this study. The docking results with rerank score as the main evaluation parameter are an important indicator in predicting the strength and stability of the interaction between GA and catalase (see Results, **Table 2**). This rerank score reflects the predicted free energy of binding with increasingly negative values indicating stronger binding and generally better ligand-receptor interactions. The results showing that GA has a higher value than the native ligand from the structure model is a reasonable result, because the native ligand may have been biochemically optimized to be able to bind with catalase, while the negative rerank score of GA towards catalase indicate the presence of a bond between them in certain levels that might trigger the targeted inhibitory activity. These results can then be used as a basis for carrying out molecular dynamics (MD) simulations and the subsequent in-vitro experiments.

Analysis of the results of redocking NADPH shows that NADPH engages with catalase through diverse type of residues—ranging from charged (Arg, His, Lys) and polar (Gln, Ser, Tyr) to non-polar (Leu, Phe, Pro, Val, Ala)— as shown in supplementary table 4, which indicates that NADPH interacts with multiple regions within the catalase active site. GA, although forming fewer interactions with catalase, still establishes hydrogen bonds and steric hindrance interactions. Key residues involved in GA binding include Arg 203, Asn 149, Gln 195, Phe 198, and Ser 201. The presence of hydrogen bonds implies that GA can form a stable complex with catalase, potentially influencing its activity. Both NADPH and GA interactions highlight the importance of Arg 203, Phe 198, and Ser 201, as potentially critical for their binding within the catalase active site. NADPH's more comprehensive interaction profile involves a larger number of amino acid residues and various interaction types, suggesting stronger and more specific binding to catalase, which is expected of the native ligand. Despite these facts, GA's interaction with key residues, despite being less extensive, indicates potential competitive inhibition with NADPH. This interaction hints at the possibility of GA modulating

catalase activity, either by occupying the binding site of NADPH or by inducing structural changes in the enzyme. These results indicate that GA can potentially bind to the catalase active site and interact with essential residues for NADPH binding. Further experimental studies, including enzyme kinetics and structural biology experiments, are essential to validate these findings and provide deeper insights into the mechanism of GA's interaction with catalase.

Direct evidence of GA's potential clinical uses are emerging, Ozan et al. and Abdullah et al. report synergy with cisplatin in HeLa cells but it comes from a small number of preclinical studies, although the broader concept that dietary polyphenols can act as chemosensitizers is more well-established. Markowska et al. provides a comprehensive review of epigallocatechin gallate (EGCG), a related polyphenol structurally connected to GA (its ester hydrolysis releases a gallic acid motif), across breast, cervical, endometrial, and ovarian cancers with the findings that beneficial effects were observed with EGCG (25 μM) and cisplatin (250 nM) and that EGCG increased sensitivity to cisplatin by regulating the expression of the copper and cisplatin influx transporter CTR1, and also acted synergistically in combination with this chemotherapeutic, including documented synergism of sequenced EGCG-curcumin-cisplatin combinations in ovarian cancer cells. This establishes precedent for polyphenol-based chemosensitization in gynecological malignancies, including cervical cancer (Markowska et al., 2025). Muntean et al.'s review of medicinal plant bioactives in gastric cancer similarly concludes that curcumin, wogonin, baicalein, and EGCG enhanced the activity of fluoropyrimidines, platinum agents, paclitaxel, doxorubicin, or related antitumor regimens in selected gastric cancer models, while cautioning that the evidence base remains heterogeneous and is constrained by variable extract standardization, incomplete dose reporting, poor bioavailability, insufficient pharmacokinetic/pharmacodynamic integration (Muntean et al., 2026). Another corroborating evidence from Hernández-Caballero et al. reviewing *Kalanchoe pinnata* that is rich in GA, caffeic acid, and quercetin, as a cancer treatment adjuvant, noting that caffeic acid enhances cisplatin cytotoxicity in ovarian carcinoma cells and that quercetin sensitizes osteosarcoma 143B cells to cisplatin and synergistically inhibited tumor growth with cisplatin in breast cancer models while reducing cisplatin-induced renal toxicity (Hernández-Caballero et al., 2022). This dual benefit mirrors the proposed rationale for GA as an adjuvant that could, in principle, allow dose reduction of cisplatin while preserving or improving antitumor efficacy.

To date, no in vivo studies or clinical trials have specifically evaluated GA monotherapy in cervical cancer models. The clinical trial landscape for natural products in cervical/HPV-related disease has focused on other compounds. Curcumin was evaluated in a phase I clinical trial with oral administration of 0.5–12 mg for 3 months in four cervical intraepithelial neoplasia (CIN) cases, demonstrating clinical safety and histological improvement in one of four cases. Indole-3-carbinol (I-3-C) showed complete regression in a placebo-controlled trial: four of eight patients on 200 mg/day and four of nine patients on 400 mg/day achieved complete regression of CIN II–III. Its derivative DIM demonstrated in a randomized double-blind placebo-controlled phase III trial (64 patients) that CIN decreased by 1–2 grades or to normal histology in 47% of subjects, with no systemic toxicities. EGCG and podophyllotoxin have also demonstrated clinical effectiveness in treating HPV-related warts (Hosseini et al., 2025; Massa et al., 2022).

A significant limitation of the present in silico and in vitro findings is the absence of robust human pharmacokinetic data for GA. The in vitro concentrations at which GA demonstrates anticancer activity may not be pharmacologically achievable through oral administration, as most natural bioactive compounds suffer from poor bioavailability and rapid degradation in vivo. Future studies should incorporate pharmacokinetic modeling and consider advanced delivery systems such as nanoparticle encapsulation to determine whether therapeutically relevant concentrations can be achieved at the tumor site. Until such data are available, the translational potential of GA in cervical cancer remains speculative.

Conclusion

Through this in-silico prediction, it can be concluded that there is indeed an apoptotic mechanism induced by GA in HeLa cervical cancer cells which can be seen through the presence of differentially expressed genes. However, it should be acknowledged that not all of these genes are significant in inhibiting cancer cell proliferation through apoptosis. Efforts have been made to narrow down the genes that are potentially most significant in this context, and those that are most likely to be influenced by GA, through a series of statistical methods and gene annotation to a curated database. Arranging signaling pathway interactions yields one gene that could be described as the most influential. The activity of the experimental compound was then validated by molecular docking against one of the signaling pathways most likely to influence the target gene based on literature research. It is hoped that this research will become a foundation for further research, to reveal the effectiveness of this compound in the treatment of cancer cells.

References

Bakrim, S., El Omari, N., El Hachlafi, N., Bakri, Y., Lee, L.-H., & Bouyahya, A. (2022). Dietary Phenolic Compounds as Anticancer Natural Drugs: Recent Update on Molecular Mechanisms and Clinical Trials. *Foods*, *11*(21), 3323. https://doi.org/10.3390/foods11213323

Chang, Y. J., Hsu, S. L., Liu, Y. T., Lin, Y. H., Lin, M. H., Huang, S. J., Ho, J. A., & Wu, L.-C. (2015). Gallic acid induces necroptosis via TNF-α signaling pathway in activated hepatic stellate cells. *PloS One*, *10*(3), e0120713. https://doi.org/10.1371/journal.pone.0120713

Chimento, A., De Luca, A., D'Amico, M., De Amicis, F., & Pezzi, V. (2023). The Involvement of Natural Polyphenols in Molecular Mechanisms Inducing Apoptosis in Tumor Cells: A Promising Adjuvant in Cancer Therapy. *International Journal of Molecular Sciences*, *24*(2), 1680. https://doi.org/10.3390/ijms24021680

Dasari, S., Bakthavachalam, V., Chinnapaka, S., Venkatesan, R., Samy, A. L. P. A., & Munirathinam, G. (2020). Neferine, an alkaloid from lotus seed embryo targets HeLa and SiHa cervical cancer cells via pro-oxidant anticancer mechanism. *Phytotherapy Research*, *34*(9), 2366–2384. https://doi.org/10.1002/ptr.6687

Dinislam, K., Shamsi, A., Tasqeruddin, S., & Shahwan, M. (2026). Dietary Polyphenols as Natural Modulators of NF - κB Signaling in Inflammation-Driven Non-Communicable Diseases: Focus on Cancer. *Food Science & Nutrition*, *14*(7), e72027. https://doi.org/10.1002/fsn3.72027

Fakhri, S., Moradi, S. Z., Yarmohammadi, A., Narimani, F., Wallace, C. E., & Bishayee, A. (2022). Modulation of TLR/NF-κB/NLRP Signaling by Bioactive Phytocompounds: A Promising Strategy to Augment Cancer Chemotherapy and Immunotherapy. *Frontiers in Oncology*, *12*, 834072. https://doi.org/10.3389/fonc.2022.834072

Gámez-García, A., Bolinaga-Ayala, I., Yoldi, G., Espinosa-Gil, S., Diéguez-Martínez, N., Megías-Roda, E., Muñoz-Guardiola, P., & Lizcano, J. M. (2021). ERK5 Inhibition Induces Autophagy-Mediated Cancer Cell Death by Activating ER Stress. *Frontiers in Cell and Developmental Biology*, *9*, 742049. https://doi.org/10.3389/fcell.2021.742049

Hasmah Abdullah, Norlida Mamat, Syahirah Sazeli, Hermizi Hapidin, Sarina Sulong, Illyana Ismail, & Deena Elsori. (2026). Upregulation of Apoptotic Protein and Migration-Inhibitory Effects of Gallic Acid and Methyl Gallate Combined with Cisplatin in HeLa Cervical Cancer Cells. *Tropical Life Sciences Research*, *37*(1), 109–131. https://doi.org/10.21315/tlsr2026.37.1.6

Hernández-Caballero, M. E., Sierra-Ramírez, J. A., Villalobos-Valencia, R., & Seseña-Méndez, E. (2022). Potential of Kalanchoe pinnata as a Cancer Treatment Adjuvant and an Epigenetic Regulator. *Molecules*, *27*(19), 6425. https://doi.org/10.3390/molecules27196425

Hosseini, M. S., Sadeqi, A., Heidari, Z., & Boozari, M. (2025). A Comprehensive Review of Biologically Active Natural Products on Human Papillomavirus (HPV) at a Glance. *Phytotherapy Research*, *39*(5), 2262–2290. https://doi.org/10.1002/ptr.8444

Indrayanto, G., Putra, G. S., & Suhud, F. (2021). Validation of in-vitro bioassay methods: Application in herbal drug research. *Profiles of Drug Substances, Excipients, and Related Methodology*, *46*, 273–307. https://doi.org/10.1016/bs.podrm.2020.07.005

Ismail, I., Kasiraja, V., & Abdullah, H. (2021). Review on anticancer potential of Quercus infectoria and its bioactive compounds. *Biomedicine*, *41*(4), 701–705. https://doi.org/10.51248/.v41i4.298

Khorsandi, K., Kianmehr, Z., Hosseinmardi, Z., & Hosseinzadeh, R. (2020). Anti-cancer effect of gallic acid in presence of low level laser irradiation: ROS production and induction of apoptosis and ferroptosis. *Cancer Cell International*, *20*(1), 18. https://doi.org/10.1186/s12935-020-1100-y

Lee, H.-L., Lin, C.-S., Kao, S.-H., & Chou, M.-C. (2017). Gallic acid induces G1 phase arrest and apoptosis of triple-negative breast cancer cell MDA-MB-231 via p38 mitogen-activated protein kinase/p21/p27 axis. *Anti-Cancer Drugs*, *28*(10), 1150–1156. https://doi.org/10.1097/CAD.0000000000000565

Li, L., Gong, Y., Xu, K., Chen, W., Xia, J., Cheng, Z., Li, L., Yu, R., Mu, J., Le, X., Xiang, Q., Peng, W., Tang, J., & Xiang, T. (2021). ZBTB28 induces autophagy by regulation of FIP200 and Bcl-XL facilitating

cervical cancer cell apoptosis. *Journal of Experimental & Clinical Cancer Research*, *40*(1), 150. https://doi.org/10.1186/s13046-021-01948-0

Li, Z., Liu, P., Yin, A., Zhang, B., Xu, J., Chen, Z., Zhang, Z., Zhang, Y., Wang, S., Tang, L., Kong, B., & Song, K. (2025). Global landscape of cervical cancer incidence and mortality in 2022 and predictions to 2030: The urgent need to address inequalities in cervical cancer. *International Journal of Cancer*, *157*(2), 288–297. https://doi.org/10.1002/ijc.35369

Liu, Z.-W., Zhang, Y.-M., Zhang, L.-Y., Zhou, T., Li, Y.-Y., Zhou, G.-C., Miao, Z.-M., Shang, M., He, J.-P., Ding, N.-, & Liu, Y.-Q. (2021). Duality of Interactions Between TGF-β and TNF-α During Tumor Formation. *Frontiers in Immunology*, *12*, 810286. https://doi.org/10.3389/fimmu.2021.810286

Markowska, A., Antoszczak, M., Markowska, J., & Huczyński, A. (2025). Role of Epigallocatechin Gallate in Selected Malignant Neoplasms in Women. *Nutrients*, *17*(2), 212. https://doi.org/10.3390/nu17020212

Massa, S., Pagliarello, R., Paolini, F., & Venuti, A. (2022). Natural Bioactives: Back to the Future in the Fight against Human Papillomavirus? A Narrative Review. *Journal of Clinical Medicine*, *11*(5), 1465. https://doi.org/10.3390/jcm11051465

Meem, P. I., Islam, Z., Eshaque, N. H., Mamun, Md. J. I., Mojidee, K. M., Badrudduja, M., Dam, A. K., & Hossen, S. M. M. (2026). Pharmacological Evaluation of Methanolic Fruit Extract of *Lannea coromandelica*: Antioxidant, Cytotoxic, Antidiabetic, Antibacterial, Anti-Inflammatory, and Sedative Activities. *Food Science & Nutrition*, *14*(5), e71858. https://doi.org/10.1002/fsn3.71858

Moghtaderi, H., Sepehri, H., Delphi, L., & Attari, F. (2018). Gallic acid and curcumin induce cytotoxicity and apoptosis in human breast cancer cell MDA-MB-231. *BioImpacts*, *8*(3), 185–194. https://doi.org/10.15171/bi.2018.21

Muntean, E. D., Lazăr, D.-C., Pah, A.-M., Banciu, C., Chiriac, S.-D., Boantă, I. D., Muntean, F., Blidişel, I.-A., Drăghici, G.-A., & Jipa, R. (2026). Synergistic Interactions Between Medicinal Plant Bioactive and Standard Chemotherapy in Gastric Cancer: Preclinical Evidence and Translational Pitfalls. *Biomedicines*, *14*(4), 947. https://doi.org/10.3390/biomedicines14040947

Ozan, E., Tuncer, M. C., & Özdemir, İ. (2026). Gallic Acid Potentiates Cisplatin Response in Cervical Cancer Cells Through Coordinated Cellular and Molecular Alterations. *Biology*, *15*(11), 825. https://doi.org/10.3390/biology15110825

Pandey, P., Lakhanpal, S., Mahmood, D., Kang, H. N., Kim, B., Kang, S., Choi, J., Choi, M., Pandey, S., Bhat, M., Sharma, S., Khan, F., Park, M. N., & Kim, B. (2025). An updated review summarizing the anticancer potential of flavonoids via targeting NF-kB pathway. *Frontiers in Pharmacology*, *15*, 1513422. https://doi.org/10.3389/fphar.2024.1513422

Pescinelli, L. M. R., Longue, M. F., De Oliveira, G. G. F. V., Thurler-Júnior, J. C., Charret, T. S., Nogueira, T. S. R., Pereira, M. T. M., Vieira, I. J. C., Abreu, L. S., Pascoal, V. D. B., & Pascoal, A. C. R. F. (2025). Eugenia uniflora L.: Analysis of Chemical Profile and Cytotoxic Action on Tumor (HeLa) and Non-Tumor Cells (NIH/3T3). *Pharmaceuticals*, *18*(8), 1199. https://doi.org/10.3390/ph18081199

Rackham, M. D., Brannigan, J. A., Rangachari, K., Meister, S., Wilkinson, A. J., Holder, A. A., Leatherbarrow, R. J., & Tate, E. W. (2014). Design and synthesis of high affinity inhibitors of Plasmodium falciparum and Plasmodium vivax N-myristoyltransferases directed by ligand efficiency dependent lipophilicity (LELP). *Journal of Medicinal Chemistry*, *57*(6), 2773–2788. https://doi.org/10.1021/jm500066b

Sarı, U., Zaman, F., Özdemir, İ., Öztürk, Ş., & Tuncer, M. C. (2024). Gallic Acid Induces HeLa Cell Lines Apoptosis via the P53/Bax Signaling Pathway. *Biomedicines*, *12*(11), 2632. https://doi.org/10.3390/biomedicines12112632

Seca, A., & Pinto, D. (2018). Plant secondary metabolites as anticancer agents: Successes in clinical trials and therapeutic application. *International Journal of Molecular Sciences*, *19*(1), 263. https://doi.org/10.3390/ijms19010263

Setiawati, D., Muchsin, W., & Sophan, A. (2026). Gynecologic cancers in low- and middle-income countries: Bridging the survival gap. *Cancer*, *132*(17), e70518. https://doi.org/10.1002/cncr.70518

Sharif, M., Mutiullah, I., Kausar, K., Khan, R., Irfan, M., Habtemariam, S., Khan, K., Quispe, C., Cho, W. C., Sharifi-Rad, J., & Calina, D. (2026). Natural Dietary Compounds Targeting NF-κB Signaling in Cancer: Implications for Nutrition-Based Prevention and Therapy. *Food Frontiers*, *7*(1), e70214. https://doi.org/10.1002/fft2.70214

Sivaprasad, U., & Basu, A. (2008). Inhibition of ERK attenuates autophagy and potentiates tumour necrosis factor-alpha-induced cell death in MCF-7 cells. *Journal of Cellular and Molecular Medicine*, *12*(4), 1265–1271. https://doi.org/10.1111/j.1582-4934.2008.00282.x

Sukocheva, O. A., Neganova, M. E., Aleksandrova, Y., Burcher, J. T., Chugunova, E., Fan, R., Tse, E., Sethi, G., Bishayee, A., & Liu, J. (2024). Signaling controversy and future therapeutical perspectives of targeting sphingolipid network in cancer immune editing and resistance to tumor necrosis factor-α immunotherapy. *Cell Communication and Signaling*, *22*(1), 251. https://doi.org/10.1186/s12964-024-01626-6

Tedasen, A., Ranjuanjit, S., Srirod, N., Bunluepuech, K., Pereira, M. D. L., Nissapatorn, V., Rattanawan, C., Sangphech, N., Boonhok, R., & Sarakul, O. (2026). Integrated Phytochemical, Network Pharmacology, and Molecular Docking Analyses of Triphala Extract Reveal Protective Effects Against H2O2-Induced Oxidative Hemolysis in G6PD-Deficient Erythrocytes. *Life*, *16*(8), 1359. https://doi.org/10.3390/life16081359

Wu, Z., Zhong, M., Liu, Y., Xiong, Y., Gao, Z., Ma, J., Zhuang, G., & Hong, X. (2022). Application of natural products for inducing ferroptosis in tumor cells. *Biotechnology and Applied Biochemistry*, *69*(1), 190–197. https://doi.org/10.1002/bab.2096

Xu, G., Yan, X., Hu, Z., Zheng, L., Ding, K., Zhang, Y., Qing, Y., Liu, T., Cheng, L., & Shi, Z. (2021). Glucocappasalin Induces G2/M-Phase Arrest, Apoptosis, and Autophagy Pathways by Targeting CDK1 and PLK1 in Cervical Carcinoma Cells. *Frontiers in Pharmacology*, *12*, 671138. https://doi.org/10.3389/fphar.2021.671138

Yuan, L., Cai, Y., Zhang, L., Liu, S., Li, P., & Li, X. (2022). Promoting Apoptosis, a Promising Way to Treat Breast Cancer With Natural Products: A Comprehensive Review. *Frontiers in Pharmacology*, *12*, 801662. https://doi.org/10.3389/fphar.2021.801662